JTTEE5 8:597-604

Design of Novel Plasma Sprayed Hydroxyapatite-Bond Coat Bioceramic Systems

R. B. Heimann

(Submitted 29 December 1998; in revised form 19 May 1999)

Bond coats based on bioinert ceramic materials such as titania and zirconia were developed to increase the adhesion strength of the coating system hydroxyapatite-bond coat to Ti-6Al-4V alloy surfaces used for hip endoprostheses and dental root implants. The bond coats improved the adhesion strength, measured by a modified ASTM D 3167-76 peel test, by up to 100% and also the resorption resistance as determined by *in vitro* leaching in simulated protein-free body fluid for up to 28 days.

Keywords adhesion strength, bond coats, hydroxyapatite coatings, peel test, reprecipitation

1. Introduction

The number of patients receiving biomedical implants to correct skeletal defects and diseases is increasing worldwide. Large demands exist for hip and knee endoprostheses, dental implants, and bone replacement parts in the maxillar-mandibular area, the ossicular chain of the inner ear, and alveolar ridge, and iliac crest augmentation. Today, more than 600,000 total hip and knee arthroplasties are being performed annually in Europe and the United States (Ref 1). One of the many problems to be solved is associated with the fact that a growing proportion of patients will outlive the expected lifetime of their prostheses. Therefore, required remediation operations that put severe physical and mental stress on patients and a high financial burden on society are increasing. Since as many as 10% of all prosthetic failures can be related to delamination of the bioactive coatings from the implant surface (Ref 2), an increase of the adhesive strength of such coatings is thought to improve their mechanical performance.

2. Substrate/Biomaterial Interface

2.1 Function of Bioactive Ceramic Coatings

The present procedure to stabilize the tissue/implant interface is through bioactive fixation with a thin plasma sprayed hydroxyapatite coating that appears to trigger bidirectional gap-healing through the occurrence of two ossification fronts, one growing from the surrounding bone toward the implant, the other from the implant to surrounding bone (Ref 3). The hydroxyapatite provides a local source for calcium and phosphate ions required for the mineralization of the surrounding tissue and also a porous template into which bone cells can grow (Ref 4). Thus, the anchoring of the implant to the surrounding living tissue is improved since the bioactive hydroxyapatite elicits a specific biological response at the interface of the material by control of its surface chemistry. The bioactive surface reacts with body fluid in a way that is compatible with the natural repair process of tissue. This results in the formation of a strong osseoconductive bond between tissue and biomaterial. Indeed, this bond can be so strong that its strength under shear loading (Ref 5) overrides the bonding of the coating to the metallic implant, and consequently a gap develops into which acellular connective issue can invade with the associated risk of aseptic loosening. The concept of a bioinert bond coat is being developed to prevent such loosening.

2.2 Function of Bioinert Bond Coats

The use of bond coats to increase the adhesion of ceramic wear- and corrosion-resistant coatings as well as thermal barrier coatings to a metallic substrate is well documented in the thermal spraying literature (Ref 6). Hence, biocompatible bond coats may offer a means to further enhance the adhesion of hydroxyapatite (HAp) coatings to metallic substrates (Ref 7). Such a bond coat should also exhibit the following properties:

- The bond coat should prevent direct contact between titanium and HAp since this is thought to catalyze thermal decomposition of HAp (Ref 8, 9).
- The bond coat should reduce or even completely prevent the release of metal ions from the Ti-6Al-4V substrate to the surrounding living tissue. Such ion release has been found to cause massive hepatic degeneration in animal experiments (Ref 10) as well as impaired development of human osteoblasts in *in vitro* tests (Ref 11) since the ions may affect the transcription of RNA in cell nuclei and influence the activity of enzymes by replacing calcium or magnesium ions at binding sites (Ref 12).
- The bond coat should reduce the thermal gradient at the substrate/coating interface induced by the rapid quenching of the molten particle splats that leads to deposition of amorphous calcium phosphate (ACP) with a concurrent decrease in resorption resistance (Ref 7) and hence to

R. B. Heimann, Chair of Technical Mineralogy, Department of Mineralogy, Freiberg University of Mining and Technology, D09596 Freiberg, Germany. Contact e-mail: heimann@mineral.tu-freiberg.de.

reduced *in vivo* performance, that is, longevity of the implants.

- The bond coat should prevent a steep gradient in the coefficients of thermal expansion (CTEs) between substrate and coating that will otherwise induce large residual tensile stresses leading to cracking and delamination of the coatings.
- The bond coat should cushion damage of the coating initiated by cyclic micromotions of the implant during movement of the patient in the initial phase of osseointegration (Ref 13).

There is evidence that even without a bond coat acting as a sink for metal ions, HAp itself effectively absorbs titanium ions released from Ti-6Al-4V implants (Ref 14), or chromium and nickel ions released from stainless steel implants (Ref 15). According to a study by Ribeiro et al. (Ref 16), calcium atoms in HAp were partially replaced by titanium atoms from a saline physiological solution of 0.9% NaCl to which titanium ions were added to simulate the release of Ti from Ti-6Al-4V. Fourier transform infrared (FTIR) and FT-Raman (FTRS) investigations suggested the formation of a titanium-substituted hydroxylapatite ($Ca_{10-n}Ti_{n/2}[(PO_4)_6(OH)_2]$.

2.3 Previous Work on Bond Coats

Yang et al. (Ref 17) investigated the system of CoCr alloy substrate/CoCr alloy bond coat/HAp. The microtextured (beaded) bond coat of 100 μm thickness was applied by plasma spraying to ensure good adhesion between the substrate and the 50 μm thick HAp top coat. It was found that the HAp coating in conjunction with a porous sinter-beaded CoCr bond coat (Ref 18) or a substrate with macrotextured grooves (Ref 19) gave significantly enhanced bone apposition and adhesive strength. In particular, the adhesive shear strength of the HAp coating increased to about 10 MPa as opposed to 1 to 2 MPa found for the bone/coating interface of macrotextured CoCr alloy substrate samples coated only with CoCr alloy beads. This is in contrast to the opinion widely held among surgeons that a strong bond to the bone can be established without an HAp layer. It is also thought that a plasma sprayed spongy titanium layer will be preferable over hydroxyapatite even though there is concern that spraying of a titanium coating on top of a Ti-6Al-4V implant may cause a dramatic decrease in high-cycle fatigue performance (Ref 20). It should be emphasized that the shear strength performance of the bone/implant interface is notoriously weak and is typically less than 40% of that of cortical bone (Ref 21).

Previous studies by Lamy et al. (Ref 22) investigated the feasibility of applying calcium silicate-based bond coats to enhance the adhesion strength and resorption resistance of the bioceramic top coat. These bond coats ought to be biocompatible since calcium silicate-glasses were found to bond easily to living bone forming an apatite surface layer when exposed to simulated body fluid (Ref 23). In addition, histological investigations provide evidence that silicon may be allied to the initiation of mineralization of preosseous tissue in periosteal or endochondral ossification (Ref 24). A dicalcium silicate bond coat yielded an as-sprayed adhesion strength of 32 MPa that on immersion in Hank's Balanced Salt Solution (HBSS) at 37 °C for 7 days decreased to 21 MPa (Ref 7). This large decrease may be due to a hydrolysis reaction of the β-dicalcium silicate formed during plasma spraying from the γ-dicalcium silicate present in the initial spray powder. It is conjectured, however, that during longer exposure to the phosphate-bearing HBSS the $Ca(OH)_2$ released during hydrolysis of β-dicalcium silicate will eventually lead to formation of very fine crystalline secondary HAp or other calcium phosphates (refer to Fig. 6) at the interface, thus strengthening the microstructure.

It is furthermore conceivable that during plasma spraying HAp and dicalcium silicate react by forming calcium silicophosphates such as silicoglaserite and/or silicocarnotite. Preliminary laser-Raman spectroscopic results point to the occurrence of such phases even though it is very difficult to distinguish between dicalcium silicate and calcium silicophosphates because of the similarity of their Raman spectra. At the interface between the bond coat and the titanium substrate calcium titanium silicate could be formed, thus establishing a chemical bond and substantially enhancing the adhesive strength of the "tandem" dicalcium silicate-HAp. In addition, calcium silicate bond coats have, for ceramics, exceptionally large CTEs ranging from 10 to 13×10^{-6}/K (Ref 25). Since the CTE of titanium is only 8.5×10^{-6}/K, there is a good match and the residual stresses (Ref 26) will be minimized. In fact, there is even the chance of introducing a compressive stress component at the interface between the substrate and the calcium silicate bond coat, thereby supporting good adhesion.

Table 1 Plasma spray conditions

Parameter	Spray set K	Spray set H
Plasma power, kW	42	26
Argon/hydrogen, L/min	40:12	50:4
Torch speed, m/min	30	30
Carrier gas flow, L/min	3	6
Powder feed rate, g/min	18.5-23	24
Stand-off distance, mm	100	100

3. Materials and Experiments

3.1 Plasma Spraying

Hydroxyapatite/bond coat systems were plasma sprayed onto Ti-6Al-4V coupons of dimension 50 by 20 by 2 mm^3 and foils of dimension 120 by 16 by 0.1 mm^3 using atmospheric plasma spray equipment (F4 plasmatron, Plasmatechnik AG, Wohlen, Switzerland) (Ref 27-29). Grit blasting of the coupons

Table 2 Composition of HBSS in 1 L deionized water

	HBSS composition, mg						
	NaCl	$CaCl_2$	KCl	$MgCl_2$	Na_2HPO_4	KH_2PO_4	$MgSO_4$
Quantity in 1 L	8,000	140	400	100	60	60	100

was performed using silicon carbide (grain size range 0.7 to 1.0 mm) at an air pressure of 500 kPa and a distance of 50 mm from the target. Grit blasting of the foils was done using alumina grit (0.6 to 0.8 mm) at an air pressure of 250 kPa and a distance of 50 mm.

Bond coats of 10 to 15 μm thickness consisted of (1) titania (grain size range 5 to 22 μm, AMDRY 6500, Sulzer Metco, Deutschland, GmbH, Hattersheim, Germany) and (2) a mechanically mixed powder of 73 mol% titania and 27 mol% zirconia (grain size range 0.18 to 26 μm, type 9303, Carl Roth GmbH, Karlsruhe, Germany), corresponding to the eutectic composition (spray parameter set K, Table 1). Subsequently, HAp coatings (150 to 180 μm thick) were applied on top of the bond coats using the H set of spray parameters (Table 1).

3.2 Sample Leaching

Five millimeter slices cut parallel to the shorter edge of the as-sprayed coupons were cleaned in acetone and methanol and immersed for 7, 14, and 28 days in 50 mL of protein-free HBSS at 37 ± 0.5 °C to study the *in vitro* resorption resistance of the various coatings systems. The ratio of the surface area of the coating to the volume of the leaching solution was 2 m^{-1}. The composition of HBSS is shown in Table 2 (Ref 30).

3.3 Sample Preparation for SEM Investigations

Two types of sample were prepared, surface and cross-sectional samples. For surface samples, 5 mm wide slices were cut parallel to the shorter edge of the coated coupons with a low-speed saw, cleaned, affixed with copper tape to the scanning electron microscope (SEM) sample holder, and coated with a thin carbon layer before mounting in the Hitachi S2700 SEM. For cross-sectional samples, the 5 by 20 mm slices were cut again in half (to 5 by 10 mm), and the two pieces glued together coating-to-coating with epoxy resin loaded with nickel powder (+20–100 μm) to maintain good edge retention during the subsequent grinding and polishing cycles. The sample sandwich was embedded in thermoplastic acrylic resin (Lucite) and the surface ground with silicon carbide paper (600 grit) using the "trailing edge" technique in which the sample is abraded only in the direction perpendicular to the edge of interest (Ref 31). This procedure is recommended for grinding of layered materials of very dissimilar hardnesses and abrasion rates such as the succession of titanium, ceramic bond coat, hydroxyapatite top coat, and epoxy resin. Polishing was performed on nylon cloth using 6 μm diamond paste, followed by a slurry of alumina on short-napped cloth.

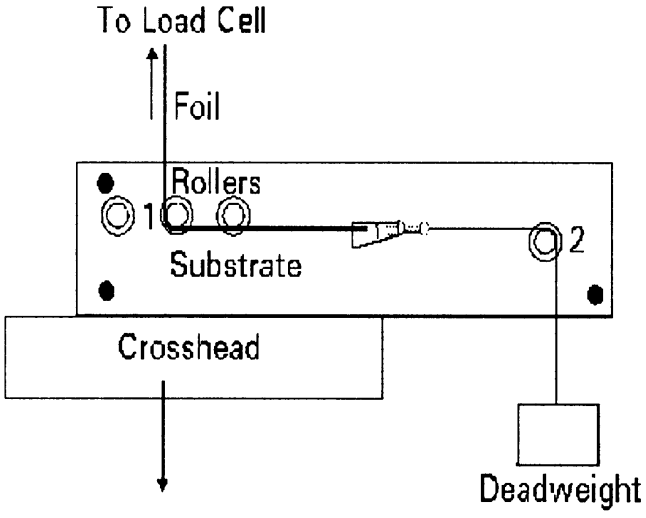

Fig. 1 Peel adhesion test loading jig with deadweight attached

3.4 Peel Adhesion Testing

The Ti-6Al-4V foils were attached to copper blocks acting as a heat sink using a 1-to-2 mixture of a silicone sealant (Dow Corning 732, Dow Corning Corp., Midland, MI) and copper powder grain size range <44 μm, ALCAN 154 (Alcan Chemicals, Brockville, ON). The adhesive was cured at ambient temperature for 12 h. After plasma spraying, the Ti-6Al-4V foils were fixed to a stiff aluminum plate (120 by 16 by 2 mm^3) with epoxy resin (HYSOL EA 934 NA, Hysol Aerospace Products, Dexter Corp., Seabrook, NH) and the copper block removed. Subsequently the assembly was mounted on a jig (Fig. 1) in an INSTRON 4200 universal testing machine (Instron Corporation, Canton, MA). The end of the foil was clamped to the upper grip of the machine and pulled away from the coating at a constant rate of 2.5 mm/min. Various deadweights were attached to the other end of the foil, and the load and the crosshead displacement digitally recorded. The stress-strain curve and the peeling force were plotted against the deadweight following the procedures of Sexsmith and Troczynski (Ref 32) and Kurzweg et al. (Ref 27, 28).

The modified ASTM D 3167-76 peel test causes a crack to propagate precisely along the coating/foil interface in a stable and controllable manner since the sample geometry forces the crack tip to move along the interface (Ref 33) where it encounters the local least energy path. Hence, it alleviates one of the problems associated with tensile pull tests such as ASTM C 633 or EN:582.93 where the uncontrolled mode of coating/substrate separation causes uncertainties concerning the value of the separated coating area to choose for calculation of the failure stress. While the tensile pull test measures this failure stress, expressed as the ratio of applied force to coating area (dimension: N/m^2), the peel test measures the energy required to separate the coating and the foil along a line (dimension: N/m). The total force (F) normalized to the width of the foil (w) is the sum of several contributions including the actual peel force (G), the deadweight (D), the frictional force (f), and the plastic work required to bend the foil per increment of peeled coating (U_b/dx). Hence the recorded force F can be represented by:

$$F = G + D + f + (U_b/dx) \quad \text{(Eq 1)}$$

Since the frictional force f can be described by $f = \mu \cdot F$, where μ is the coefficient of rolling friction, and the plastic work of bending is a function of the applied force and also proportional to the width of the foil, w, Eq 1 can be rewritten as:

$$F(1 - \mu) = G + D + \alpha w \quad \text{(Eq 2)}$$

where α is the plastic work expended per unit width per unit length that can be determined from the stress-strain curve of the uncoated titanium alloy foil.

4. Results and Discussion

4.1 Plasma Sprayed Coatings

Cross sections of the plasma sprayed coatings were prepared as described above and investigated by SEM. Figure 2 shows a largely continuous interface of the titania bond coat (center) to both the Ti-6Al-4V alloy implant material (left) and the hydroxyapatite coating (right) suggesting improved mechanical performance of the system.

Similar results were obtained for systems with a mixed titania-zirconia bond coat. The porosity of 5 to 10% of the hydroxyapatite top layer appears to be sufficient to allow unimpeded growth of bone cells into the layer to facilitate bone apposition.

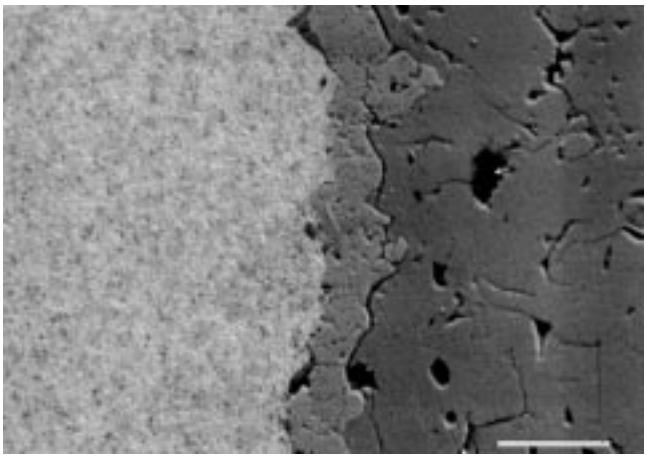

Fig. 2 SEM photomicrograph of a cross section of a titania bond coat/hydroxyapatite top coat system (Ti-6Al-4V). Left: substrate, light gray; center: titania bond coat, medium gray; right: hydroxyapatite, dark gray

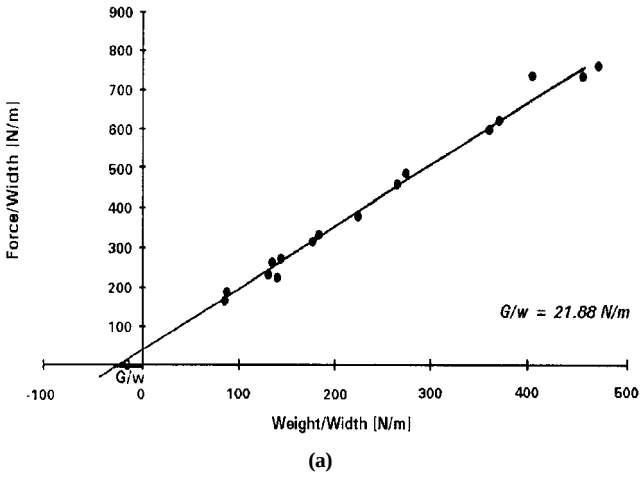

(a)

Fig. 3(a) Plot of the total force versus the deadweight to determine the peel adhesion strength of a HAp coating without a bond coat. All quantities were related to the width of the foil, *w*.

4.2 Adhesion Strength of Coatings

Figures 3(a) and (b) show the total force plotted against the deadweight from which lines the peel strengths of a HAp coating without a bond coat (Fig. 3a) and a HAp/titania bond coat system (Fig. 3b) were calculated to be 21.9 and 42.1 N/m, respectively. All quantities were related to the width of the foil, *w*. A significance test (t-test) was done based on the comparison of the intersection with the negative *x*-axes. The calculated $|t_r^{(a)}|$ values are higher than the tabulated $t_{\nu,q}$ values for ν degrees of freedom and a level of confidence $\alpha = 0.05$ (Table 3), thus rejecting the null hypothesis that the true means of the peel strengths of the different systems are equal.

To confirm these findings, conventional tensile adhesion tests (EN:582.93) were performed on Ti-6Al-4V cylinders (25 mm diameter, 55 mm length) coated with HAp without a bond coat as well as a HAp/titania bond coat system. The cylinders were grit blasted and plasma sprayed under identical conditions as the foils and the coupons. The adhesive used was HTK Ultrabond 100 (HTK Hamburg GmbH, Germany) with a maximum adhesion strength of 100 MPa. The average value (n = 3) of the adhesion strength (failure stress) of HAp on Ti-6Al-4V was found to be 37 ± 3 MPa, that of HAp + TiO_2 bond coat 45 ± 3 MPa. Separation occurred always at the interface of HAp with the alloy substrate and the TiO_2 bond coat, respectively.

Thus, it can be concluded that the adhesion strengths of the bioceramic coating systems in the presence of bond coats consisting of either zirconia/titania or titania are significantly

Table 3 Calculated peel strengths

System	Peel strength, N/m	Calculated, $\lvert t_r^{(a)} \rvert$	Tabulated, $t_{\nu,q}$
HAp	21.9	…	…
HAp/ZrO_2 + TiO_2	31.8	2.15	2.06
HAp/TiO_2	42.1	2.67	2.07

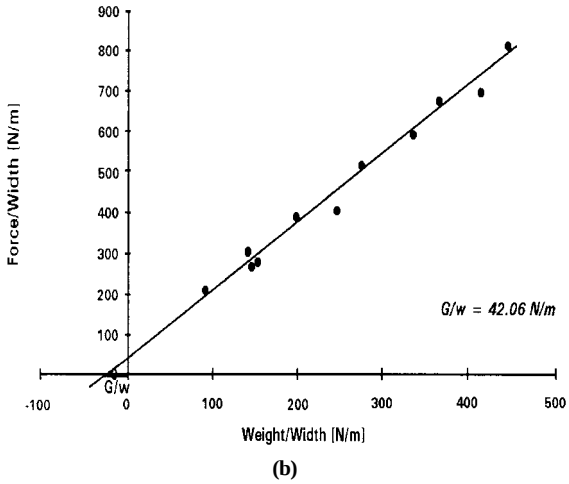

(b)

Fig. 3(b) Plot of the total force versus the deadweight to determine the peel adhesion strength of a HAp/TiO_2 coating system. All quantities were related to the width of the foil, *w*.

increased compared to HAp coatings without a bond coat, plasma sprayed and tested under identical conditions. The reason for this may be that the bond coats act as natural extensions of the very thin oxide layer that naturally covers a titanium metal surface.

On the other hand, since the metal/bioceramic interface is designed to facilitate unimpeded transmission of load from the implant to the surrounding bone, and since shear-induced micromotions during the early healing phase may lead to disruption of the otherwise tightly adhering passive oxide layer, a thick titania bond coat may act to prevent coating delamination by acting as a buffer against undue release of titanium ions that can induce a cytotoxic response, as well as a sound anchoring substrate for hydroxyapatite. There is a good match between the CTE of the titanium alloy (8.5×10^{-6}/K), the bond coat (8.2×10^{-6}/K for zirconia/titania and 7.5×10^{-6}/K for titania, respectively) and the HAp top coat (11×10^{-6}/K, Ref 34). Hence there are very little if any stresses due to thermal mismatch present at the metal substrate/bond coat interface, and weak compressive stresses at the bond coat/HAp top coat interface. Both facts suggest favorable conditions for well-adhering coating systems notwithstanding the fact that additional residual stresses will be present, caused by strong particle shrinkage (Ref 35) due to the high CTE of HAp.

Whether a chemical reaction zone exists between titania and HAp, consisting for example of a very thin calcium titanate (perovskite, Ref 36) or calcium dititanate layer (Ref 8), or a titanium-substituted hydroxyapatite as suggested by Ribeiro et al. (Ref 16) is still a matter of conjecture to date.

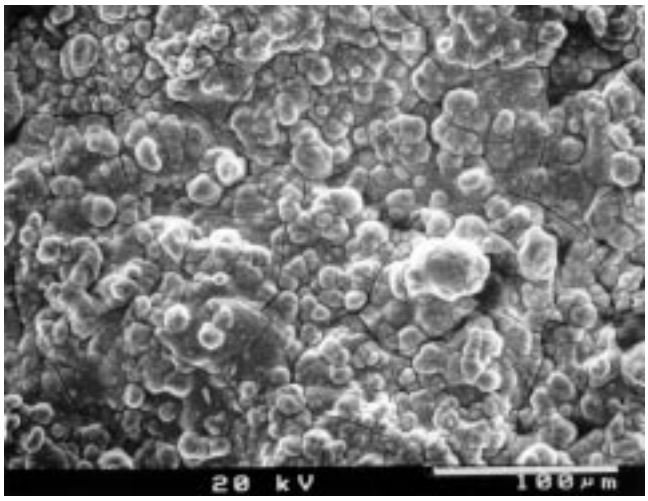

(a)

Fig. 4(a) Surface of HAp coating with a bond coat consisting of a eutectic mixture of zirconia and titania leached in HBSS for 28 days

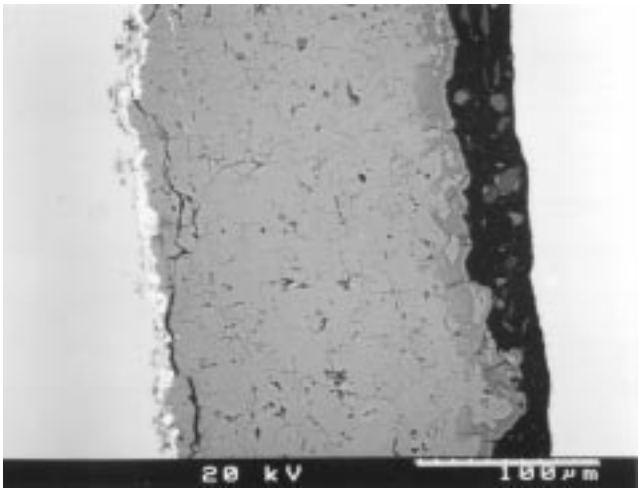

(b)

Fig. 4(b) Cross section of the sample shown in Fig. 4(a) showing from left to right the Ti-6Al-4V substrate (light, extreme left), the TiO_2/ZrO_2 bond coat, the HAp layer (light gray, center), its leached outer portion (dark gray), the epoxy layer (black, right) and a titanium strip used to aid in sample preparation (white, extreme right)

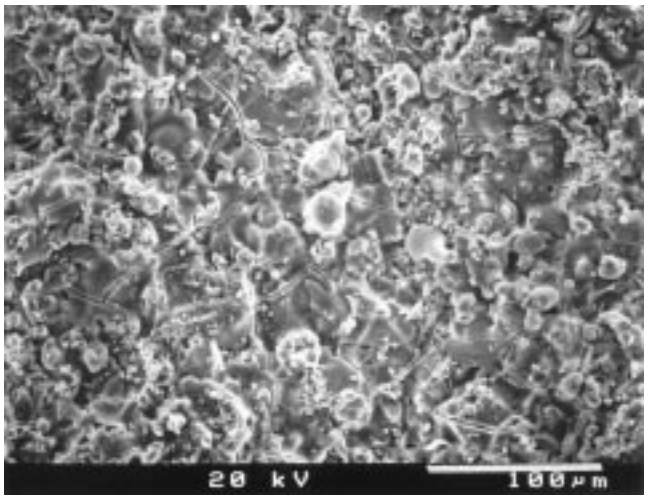

(a)

Fig. 5(a) Surface of a HAp coating with a titania bond coat leached in HBSS for 28 days

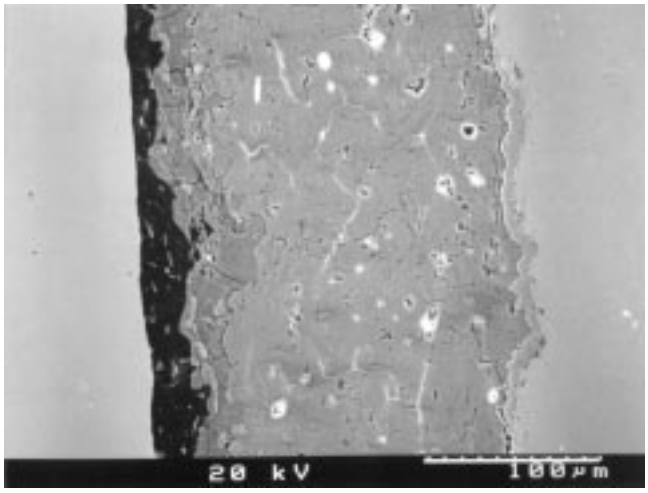

(b)

Fig. 5(b) Cross section of a HAp/TiO_2 system leached in HBSS for 28 days. From left to right: Ti strip (light gray) used to aid in sample preparation, epoxy resin (black), HAp (medium gray, center), TiO_2 bond coat (light gray), and Ti-6Al-4V substrate (gray, right)

4.3 Microstructure of Leached Coatings

Figures 4 and 5 show SEM micrographs of surfaces and cross sections, respectively, of the coating systems HAp/ZrO_2 + TiO_2 (Fig. 4) and HAp/TiO_2 (Fig. 5) leached in HBSS for 28 days. Figure 4a shows the HAp surface with a characteristic microstructure akin to a "cauliflower" pattern suggesting precipitation of calcium phosphate/hydroxyapatite from the leaching solution. This finding is equivalent to the precipitation of poorly crystallized "bonelike" apatite reported by Weng et al. (Ref 37) as the product of treatment of HAp coatings in a protein-free simulated body fluid. Similar results were obtained by LeGeros et al. (Ref 38) during study of the dissolution behavior of powdered calcium phosphate materials in acidic potassium acetate buffer (pH = 5), fetal bovine serum, and in contact with cultured human bone cells in Eagle's medium. In this study, microcrystals consisting of carbonate apatite were observed that were intimately associated with a noncollageneous organic matrix.

In the case of plasma sprayed calcium phosphates, preferential dissolution of amorphous calcium phosphate (ACP), generated by rapid quenching of molten HAp particles impinging at the titanium alloy surface, provides the supersaturation required for heterogeneous nucleation of hydroxyapatite.

The leaching process can be followed by observing the change in the Ca/P ratio at the interface hydroxyapatite/solution (Fig. 4b). An approximately 20 μm wide leached layer appears as a dark gray zone with a Ca/P ratio of 1.28 as compared to an averaged ratio of 1.47 measured by electron-dispersive x-ray (EDX) for the lighter unaltered bulk HAp phase.

There is also a suggestion that calcium phosphate initially reprecipitates in well-developed crystals at the surface of the plasma sprayed HAp coating as shown in Fig. 6. The composition of these crystals is as follows: 19 at.% Ca, 15 at.% P, and 66 at.% O. This composition resembles that of octacalcium phosphate $Ca_8H_2(PO_4)_6 \cdot 5H_2O$ (20.0 at.% Ca, 15.0 at.% P, 60.0 at.% O, 5.0 at.% H) that is known to transform easily *in vitro* into hydroxyapatite by taking up additional CaO (Ref 39).

Figure 5(a) shows the leached HAp surface of a sample with a titania bond coat. Compared to Fig. 4(a), the surface appears much smoother with moderate cracking that does not seem to compromise the general cohesiveness of the plasma sprayed layer. There is no discernible "cauliflower" microstructure that in the system HAp/ZrO_2 + TiO_2 was attributed to precipitation of calcium phosphate from the leaching solution. Hence, the formation of ACP produced by quenching of the molten HAp particles was suppressed owing to differing heat transfer conditions into the metallic substrate induced by the bond coat acting as a thermal barrier. The differing heat transfer conditions are presumably not related to differences in the thermal conductivities since they are comparable for both types of bond coat: λ_m(200 °C) = 0.73·λ (TiO$_2$) + 0.23·λ (ZrO$_2$) = 6.5 W/m · K and λ(TiO_2,200 °C) = 7 W/m · K, but may be due to differences in the porosity of the bond coats. Spherical particles attached to the surface of the leached HAp, shown in Fig. 5(a), consist of highly crystalline hydroxyapatite as confirmed by XRD measurements.

Figure 5(b) shows the cross section of a leached sample with a titania bond coat. The bond coat (medium gray, right) appears to adhere tightly to the Ti-6Al-4V substrate (light gray, far right) as well as to the hydroxyapatite top coat (dark gray, center). The HAp layer shows a pronounced lamellar structure as well as cracks that are considered the result of mechanical load during sample preparation, that is, cutting, grinding, and polishing. The outermost portion of the HAp coating displays a leached layer of about 15 μm thickness with a Ca/P ratio of 1.27 as opposed to the bulk phase with a Ca/P ratio of 1.40. As expected, the bond coats are highly stable against leaching. Indeed, the amounts of both titanium and zirconium measured by inductively coupled plasma mass spectroscopy in the HBSS after immersion for 28 days remained below the detection limit of 5 ng/L.

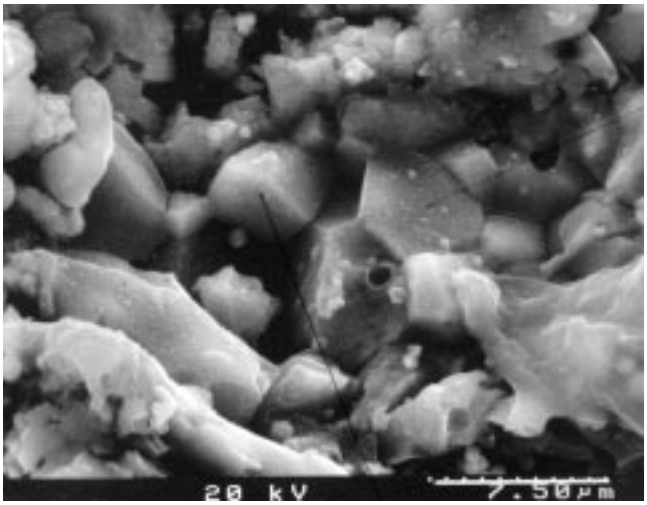

Fig. 6 Well-crystallized octacalcium phosphate reprecipitated from the leaching solution

5. Conclusions

Atmospheric plasma spraying of bioinert ceramic bond coats of zirconia/titania (eutectic composition) and titania increases the peel adhesion strength of the coating systems by 50 and 100%, respectively, when compared to hydroxyapatite coatings without a bond coat sprayed and tested under identical conditions.

The coating systems perform well to leaching in simulated protein-free body fluid (HBSS) for up to 28 days. Thin (<20 μm) layers formed during leaching of hydroxyapatite show depletion of calcium. Owing to the reduced heat transfer conditions at the bond coat/HAp top coat interface, formation of ACP was presumably suppressed, and hence leaching was reduced in systems with bond coats compared to those consisting of hydroxyapatite only. This latter contention has still to be confirmed by additional experimental studies.

Acknowledgment

The author is much indebted to Ms. Heidi Kurzweg, Surfatec GmbH, Zschornewitz, Germany, and Dr. Tuan Anh Vu, Westerwald Industriekeramik GmbH, Wirges, Germany, for providing experimental support, and to Professor Tom Troczynski, Department of Metals and Materials Engineering, University of British Columbia, Vancouver, B.C., Canada, for granting access to his peel adhesion testing equipment. Thanks are also due to Professor Michael L. Wayman, Department of Chemical and Materials Engineering, University of Alberta, Edmonton, for assistance with the leaching studies. The work was partly supported by

a research grant of the Saxon State Ministry of Science and the Arts, Dresden, Germany, under contract No. 4-7541.82-0390/414. In addition, the author thanks the German Federal Ministry of Education, Research, Science and Technology (BMBF) for supporting a sabbatical sojourn from June to October 1996 at the University of Alberta, Edmonton, Alberta, Canada, under the auspices of the Germany/Canada Science and Technology Cooperation Program (project WTZ KAN-MPT 24).

References

1. B. Barden, Failure Mechanisms in Total Hip and Knee Arthroplasty, *Proc. Biomaterials: Fundamentals and Clinical Appl.* (Essen, Germany), 8-9 Oct 1998, p 44
2. G. Willmann, Survival Rate and Reliability of Ceramic Femoral Heads for Total Hip Arthroplasty, *Mater.wiss. Werkst.tech.*, Vol 29, 1998, p 595-604 (in German)
3. K. Soballe, H.B. Rasmussen, E.S. Hansen, and C. Buenger, Hydroxyapatite Coating Modifies Implant Membrane Formation. Controlled Micromotion Studies in Dogs, *Acta Orthop. Scand.*, Vol 63 (No. 2), 1992, p 128-140
4. J. Beight, S.R. Radin, J. Cuckler, and P. Ducheyne, Effect of Solubility of Calcium Phosphate Coatings on Mechanical Fixation of Porous Ingrown Implants, *Trans. 35th Annual Meeting Orthop. Res. Soc.*, Vol 14, 1989, p 334-342
5. R.T. Müller and T. Patsalis, Shear and Tensile Strength of Hydroxyapatite Coating under Loading Conditions. An Experimental Study in Dogs, *Arch. Orthop. Trauma Surg.*, Vol 116, 1997, p 334-337
6. R.B. Heimann, *Plasma Spray Coating. Principles and Applications*, VCH Weinheim, 1996, 339 pages
7. R.B. Heimann, T.A. Vu, and M.L. Wayman, Bioceramic Coatings: State-of-the-Art and Recent Development Trends, *Eur. J. Mineral.*, Vol 9, 1997, p 597-615
8. J. Weng, X. Liu, X. Zhang, and X. Ji, Thermal Decomposition of Hydroxyapatite Structure Induced by Titanium and its Dioxide, *J. Mater. Sci. Lett.*, Vol 13, 1994, p 159-161
9. H. Ji, C.B. Ponton, and P.M. Marquis, Microstructural Characterization of Hydroxyapatite Coatings on Titanium, *J. Mater. Sci.: Mater. Med.*, Vol 3, 1992, p 283-287
10. M.L. Pereira, A.M. Abreu, J.P. Sousa, and G.S. Carvalho, Chromium Accumulation and Ultrastructural Changes in the Mouse Liver by Stainless Steel Corrosion Products, *J. Mater. Sci.: Mater. Med.*, Vol 6, 1995, p 523-527
11. H. Tomas, G.S. Carvalho, M.H. Fernandes, A.P. Freire, and L.M. Abrantes, Effect of CoCr Corrosion Products and Corresponding Separate Metal Ions on Human Osteoblast-Like Cell Cultures, *J. Mater. Sci.: Mater. Med.*, Vol 7, 1996, p 291-296
12. H.A. Schroeder, Trace Metals and Chronic Diseases, *Adv. Int. Med.*, Vol 8, 1965, p 159-303
13. K. Soballe, Hydroxyapatite Ceramics for Bone Implant Fixation. Mechanical and Histological Studies in Dogs, *Acta Orthop. Scand.*, Vol 64 (No. 255), 1993, 58 pages
14. P. Ducheyne and K.E. Healy, The Effect of Plasma-Sprayed Calcium Phosphate Ceramic Coatings on Metal Ion Release from Porous Titanium and Cobalt-Chromium Alloy, *J. Biomed. Mater. Res.*, Vol 22, 1988, p 1137-1163
15. S.R. Sousa and M.A. Barbosa, The Effect of Hydroxyapatite Thickness on Metal Ions Release from Stainless Steel Substrates, *J. Mater. Sci.: Mater. Med.*, Vol 6, 1995, p 818-823
16. C.C. Ribeiro, M.A. Barbosa, A.A.S.C. Machado, A. Tudor, and M.C. Davies, Modification in the Molecular Structure of Hydroxyapatite Induced by Titanium Ions, *J. Mater. Sci: Mater. Med.*, Vol 6, 1995, p 829-834
17. C.Y. Yang, B.C. Wang, W.J. Chang, E. Chang, and J.D. Wu, The Influence of Plasma Spraying Parameters on the Characteristics of Hydroxyapatite Coatings: A Quantitative Study, *J. Mater. Sci.: Mater. Med.*, Vol 7, 1996, p 167-174
18. J.C. Chae, J.P. Collier, M.B. Mayor, V.A. Surprenant, and L.A. Dauphinais, Enhanced Ingrowth of Porous-Coated CoCr Implants Plasma-Sprayed with Tricalcium Phosphate, *J. Biomed. Mater. Res.*, Vol 26, 1992, p 93-102
19. K.A. Thomas, J.F. Kay, S.D. Cook, and M. Jarcho, The Effect of Surface Macrotexture and Hydroxyapatite Coating on the Mechanical Strength and Histological Profiles of Titanium Implant Materials, *J. Biomed. Mater. Res.*, Vol 21, 1987, p 395-414
20. T. Smith, The Effect of Plasma-Sprayed Coatings on the Fatigue of Titanium Alloy Implants, *J. Mater.*, Feb 1994, p 54-56
21. R.G.T. Geesink, K. de Groot, and C.P.A.T. Klein, Chemical Implant Fixation Using Hydroxyapatite Coatings, *Clin. Orthop. Rel. Res.*, Vol 225, 1987, p 147-170
22. D. Lamy, A.C. Pierre, and R.B. Heimann, Hydroxyapatite Coatings with a Bond Coat on Biomedical Implants by Plasma Projection, *J. Mater. Res.*, Vol 11 (No. 3), 1996, p 680-686
23. Y. Ebisawa, T. Kokubo, K. Ohura, and T. Yamamuro, Bioactivity of CaO SiO_2-Based Glasses: In Vitro Evaluation, *J. Mater. Sci.: Mater. Med.*, Vol 1, 1990, p 239-244
24. E.M. Carlisle, Silicon: A Possible Factor in Bone Calcification, *Science*, Vol 167, 16 Jan 1970, p 279-280
25. K. Ogawa, N. Nagata, and T. Yogoro, *Onoda Res. Rep.*, Vol 43, 2nd book (No. 125), 1991, p 46-54 (in Japanese)
26. S.R. Brown, I.G. Turner, and H. Reiter, Residual Stress Measurements in Thermal Sprayed Hydroxyapatite Coatings, *J. Mater. Sci.: Mater. Med.*, Vol 5, 1994, p 756-759
27. H. Kurzweg, T. Troczynski, and R.B. Heimann, Adhesion of Thermally Sprayed Hydroxyapatite-Bond-Coat Systems Measured by a Novel Peel Test, *J. Mater. Sci.: Mater. Med.*, Vol 9, 1998, p 9-16
28. H. Kurzweg, R.B. Heimann, T. Troczynski, and M.L. Wayman, Development of Plasma-Sprayed Bioceramic Coatings with Bond Coats Based on Titania and Zirconia, *Biomaterials*, Vol 19, 1998, p 1507-1511
29. R.B. Heimann, H. Kurzweg, and T.A. Vu, Hydroxyapatite-Bond Coat Systems for Improved Mechanical and Biological Performance of Hip Implants, *Thermal Spray: Meeting the Challenges of the 21st Century*, C. Coddet, Ed., 25-29 May 1998, Nice, France, p 999-1005
30. O. Ohtsuka, M. Matsura, N. Chida, M. Yoshinori, T. Sumii, and T. Dérand, Formation of Hydroxyapatite on Pure Titanium Substrates by Ion Beam Dynamic Mixing, *Surf. Coat. Technol.*, Vol 65, 1994, p 224-230
31. L.E. Samuels, *Metallographic Polishing by Mechanical Methods*, American Society for Metals, 1982, p 288
32. M. Sexsmith and T. Troczynski, Peel Adhesion Test for Thermal Sprayed Coatings, *J.Therm. Spray Technol.*, Vol 3 (No. 4), 1994, p 404-409
33. A.D. Crocombe and R.D. Adams, Peel Analysis Using the Finite Element Method, *J. Adhes.*, Vol 12, 1981, p 127-139
34. G. Willmann, Material Properties of Hydroxylapatite Ceramics, *Interceram*, Vol 42 (No. 4), 1993, p 206-208
35. T.W. Clyne and S.C. Gill, Residual Stresses in Thermal Spray Coatings and Their Effect on Interfacial Adhesion: A Review of Recent Work, *J. Therm. Spray Technol.*, Vol 5 (No. 4), 1996, p 401-418
36. K. de Groot, R.T.G. Geesink, C.P.A.T. Klein, and P. Serekian, Plasma-Sprayed Coatings of Hydroxyl-Apatite, *J. Biomed. Mater. Res.*, Vol 21, 1987, p 1375-1381
37. J. Weng, Q. Liu, J.G.C. Wolke, D. Zhang, and K. de Groot, *J. Mater. Sci. Lett.*, Vol 16, 1997, p 335-337
38. R.Z. LeGeros, I. Orly, M. Gregoire, and G. Dalcusi, Substrate Surface Dissolution and Interfacial Biological Mineralization, *The Bone-Biomaterial Interface*, J.E. Davies, Ed., University of Toronto Press, 1991, p 76-88
39. R.Z. LeGeros, G. Dalcusi, I. Orly, T. Abergas, and W. Torres, Solution-Mediated Transformation of Octacalcium Phosphate (OCP) to Apatite, *Scan. Microsc.*, Vol 3, 1989, p 129-138